NANO LETTERS

pubs.acs.org/NanoLett Letter

Flexible and Robust Three-Dimensional Covalent Organic Framework Membranes for Precise Separations under Extreme Conditions

Xiansong Shi, Zhe Zhang, Siyu Fang, Jingtao Wang, Yatao Zhang, and Yong Wang*

Cite This: *Nano Lett.* 2021, 21, 8355−8362 Read Online

ACCESS | Metrics & More | Article Recommendations | Supporting Information

ABSTRACT: Membranes based on covalent organic frameworks (COFs) have demonstrated huge potential to resolve the long-standing bottlenecks in separation fields due to their structural and functional attributes. Herein, a three-dimensional COF featuring interpenetrated apertures, 3D-OH-COF, is rationally synthesized on polyimide supports to generate flexible, robust membranes. The resultant 3D-OH-COF presents excellent crystallinity, prominent porosity, and exceptional solvent resistance, enabling the produced membrane a sharp and durable selectivity to small molecules in water and organic solvents. Impressively, the membrane also exhibits excellent flexibility and robustness as verified by the well-maintained performances after serious bending and solvent soaking under elevated temperatures. We further chemically convert 3D-OH-COF into the carboxyl-decorated 3D-COOH-COF by a postsynthetic strategy. The 3D-COOH-COF retains high crystallinity, and the converted membrane receives a remarkable capture ability for targeted multivalent ions over other competing ions. This study exploits a viable avenue to produce practical 3D COF membranes toward ultimate separations under extreme conditions.

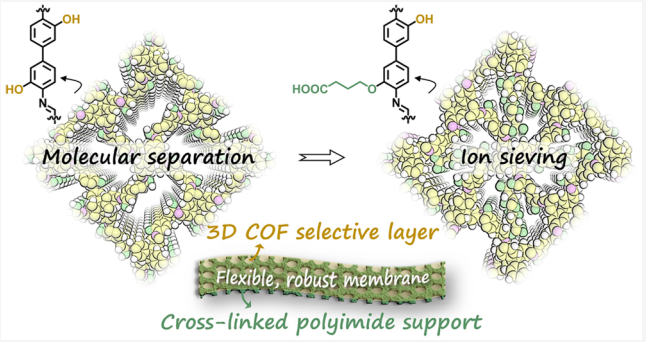

KEYWORDS: *3D COFs, chemical conversion, separation membrane, molecular separation, ion sieving*

1. INTRODUCTION

Covalent organic frameworks (COFs) represent a large family of crystalline perforated polymers, which consist of periodically connected organic building blocks through covalent linkages.[1−3] According to the dimensionality of linkages, COFs can be categorized as two-dimensional (2D) and three-dimensional (3D) types following the design principles of reticular chemistry.[4] Thanks to their ordered and tunable aperture sizes, well-defined channels, and devisable functions, COFs have emerged as a fascinating material to build powerful platforms for various demands.[3] Particularly, membranes constructed by COFs have shown a remarkable superiority to tackle the long-standing bottlenecks in separation fields, including the trade-off between permeability and selectivity as well as the limited stability.[5−8] However, regardless of those successes, the exploration of practical COF membranes is still in its infancy. As for the design of eligible COF membranes, the following vital essentials need to be seriously considered: (1) crystallinity, (2) aperture size, (3) functionality, and (4) practicability. The crystallinity of COF membranes represents the pore uniformity, which is of great importance for boosting permselectivity. To date, attempts on synthesizing COF membranes by diverse strategies have been extensively reported.[9,10] Unfortunately, the majority of the membranes demonstrate moderate crystallinity,[11−13] while the COF layers having prominent crystallinity are rarely developed. The insufficient crystallinity will degrade the separation accuracy and structural durability due to the intramolecular defects, resulting in undesired performances. Thus, developing highly crystalline COF membranes is a prerequisite to fully exert the advantages of COF materials.

Another hindrance that retards the progress of COF membranes is their relatively large aperture sizes.[6] Up to now, more than 95% of COF membranes are constituted by 2D COFs, giving effective sieving pore sizes in the range of ∼1−2.5 nm. They are probably qualified for liquid molecular separations but are incapable of treating the ionic and gaseous systems[14,15] of which the subnanometer pores are generally required. To change the situation, the accurate control over the pore size and functionality of 2D COF membranes is profoundly studied through monomer design, structural regulation, and chemical modification.[10] 3D COFs, as a

Received: July 29, 2021
Revised: August 31, 2021
Published: October 1, 2021

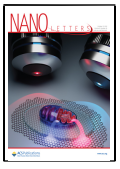

https://doi.org/10.1021/acs.nanolett.1c02919
Nano Lett. 2021, 21, 8355−8362

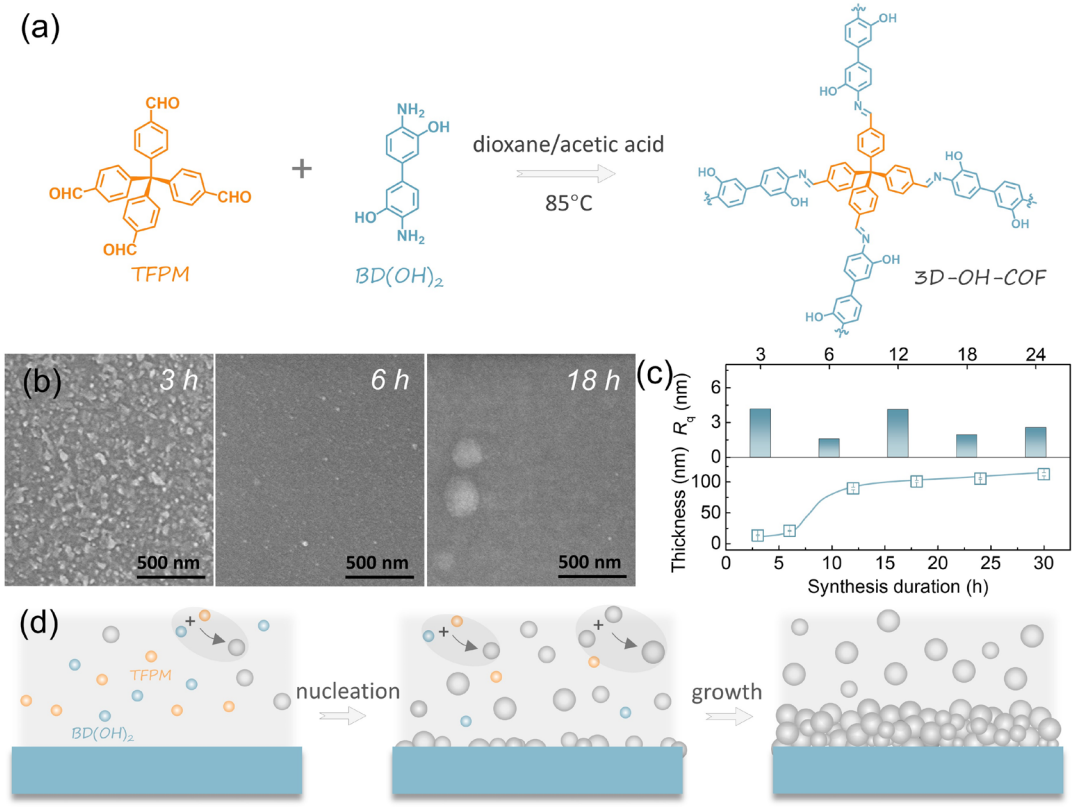

Figure 1. Investigation on the formation of 3D-OH-COF films. (a) Reaction scheme of 3D-OH-COF. (b) Surface SEM images of the films synthesized for various durations. (c) Film roughness and thickness as a function of the synthesis duration. (d) Schematic diagram of the film formation.

subfamily of COFs, are built of stereoscopic nodes and planar linkers to present an extended, interpenetrated network.[16,17] The spatial connectivity of covalent bonds unlocks a largely narrowed cavity, thus offering a facile avenue to customize angstrom-level channels.[4] Also, 3D COFs exhibit additional mass transfer pathways due to the interconnected pores, making the performance improvement much easier as compared with 2D COFs. With these benefits, 3D COFs are seen as promising candidates to prepare the prospective membranes for high-resolution separations. However, the relevant study is still technically challenging, despite the pioneering works in expanding monomers and analyzing structures.[18−20]

The rational design of supports is vital for the performance maximization and practicability promotion of separation membranes.[21,22] Nowadays, some efforts have been dedicated to growing COFs on the top of inorganic supports.[23,24] Nevertheless, these supports are usually fragile and produced at the expense of costly and time-consuming processes, limiting the large-scale production and universal applicability. Alternatively, the supports derived from polymers own excellent processability and adaptability and are generally cheaper than inorganic counterparts.[22] Therefore, the growth of high-quality COFs on polymeric supports, especially highly practical ones, benefits for the large-area production and industrial application. With these in mind, we targeted polyimide (PI), a class of widely used engineering plastics.[25] The cross-linked PI (CPI) delivers extraordinary orgainc solvent tolerance, high-temperature durability, and good mechanical strength,[26−28] making it highly viable for growing and supporting COFs.

Herein, we report the synthesis of 3D-OH-COF on mesoporous CPI supports via solvothermal growth. The 3D-OH-COF membranes show high crystallinity and narrowed pore sizes, empowering an upgraded selectivity toward small molecules. The pure organic component coupled with crystalline 3D-OH-COF endows the resultant membranes with excellent flexibility and robustness, which are tolerable for bending and solvent soaking. We further realize the chemical conversion of 3D-OH-COF into 3D-COOH-COF through the ring-opening reaction. The obtained 3D-COOH-COF membrane presents retained crystallinity and angstrom-sized pores with the carboxyl-containing pendants. The alliance of chemical and electrostatic interactions and size-dependent repulsion significantly improves the selectivity of target ions over competing ions.

2. RESULTS AND DISCUSSION

2.1. Growth of 3D-OH-COF films. As shown in Figure 1a, tetrakis(4-formylphenyl)-methane (TFPM) is used as the tetrahedral monomer to offer a 4-connected node. 3,3′-Dihydroxybenzidine ($BD(OH)_2$) is elaborately selected as a linear linker that comprises hydroxyl groups available for postsynthetic modification. Given the formation of 3D COF films is yet to be disclosed, we started with the film growth on silicon wafers under solvothermal conditions. As shown in the scanning electron microscopy (SEM) images, a short synthesis duration of 3 h produces discontinuous films with an uneven surface (Figures 1b and S3). Extending the duration to 6 h generates defect-free, continuous 3D-OH-COF films with a smooth surface, stating that the growth of 3D-OH-COF preferentially occurs at the sunken area to minimize the surface

https://doi.org/10.1021/acs.nanolett.1c02919
Nano Lett. 2021, 21, 8355−8362

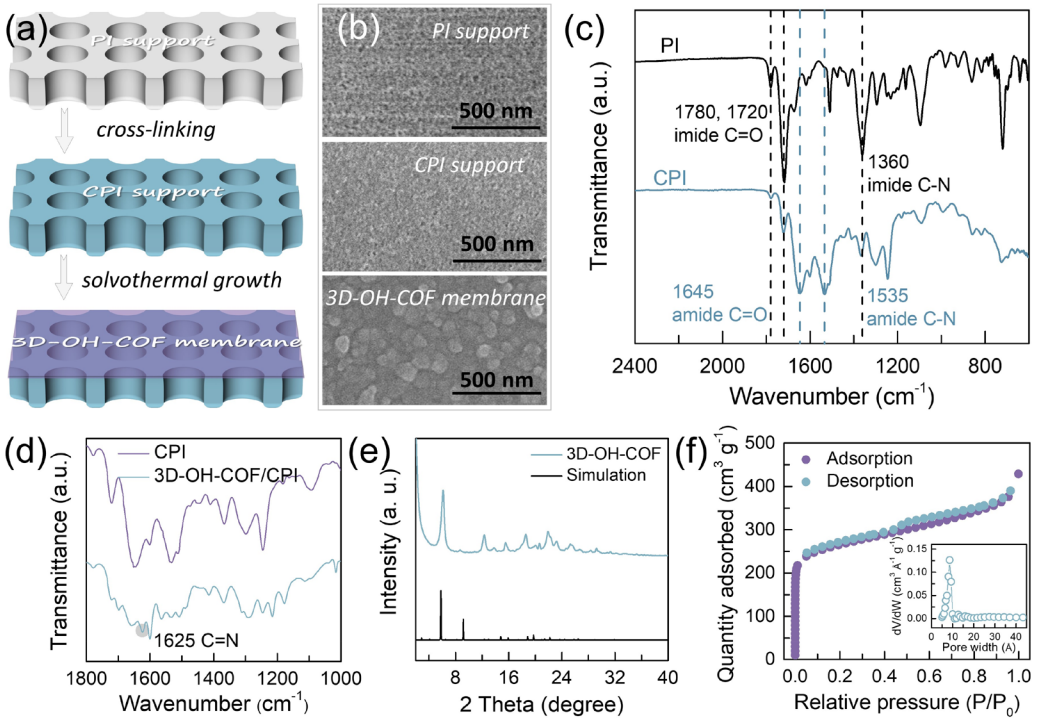

Figure 2. Characterization on the 3D-OH-COF membrane and powder synthesized for 24 h. (a) Schematic diagram of the membrane preparation. (b) Surface SEM images of the PI, CPI, and 3D-OH-COF membrane. (c,d) FTIR spectra of the PI, CPI, and 3D-OH-COF membrane. (e) Experimental and simulated XRD patterns of the powder. (f) N_2 adsorption−desorption isotherms of the powder. Inset in (f) shows the pore size distribution.

energy. The morphological features of films then keep basically unchanged with further prolonged synthesis durations (Figures 1b and S4). Atomic force microscopy (AFM) studies of films reveal a low surface roughness throughout the synthesis period of 24 h (Figures 1c and S5). The spectroscopic ellipsometry was performed to accurately determine the film thickness. With the duration extended from 3 to 6 h, the thickness slightly increases by ∼8 nm (Figure 1c), confirming the preferential growth of 3D-OH-COF at sunken locations. Subsequently, the thickness attains a sharp increase followed by raising slowly when the synthesis duration is prolonged from 12 to 30 h. On the basis of these results, we speculate the formation of 3D-OH-COF films as follows. The solvothermal condition facilitates the condensation between monomer pairs, thus producing massive crystallites dispersed in the bulk solution. The exposed hydroxyl groups on silicon wafers will then work as the active sites to anchor the resulting crystallites, and this is the time that the surface nucleation proceeds (Figure 1d).[29] Next, the crystallites tend to coalesce with their neighbors to form bigger crystals through the breaking and rebonding of imine linkages because of the reversibility of Schiff-base reaction.[30] The crystals together with crystallites will simultaneously deposit on the substrate, enabling the horizontal growth of 3D-OH-COF to produce continuous films. The escalating accumulation of crystals on the film is responsible for the vertical growth to give a continuously increased thickness. It is worth noting that the growth of 3D COF films slightly differentiates from 2D COF films. Specifically, the latter grows with the synergy of the intramolecular covalent bonds and the perpendicular $\pi-\pi$ stacking among layers.[31] The ectopic structure is often involved in 2D COFs,[32] which may compromise pore uniformity leading to nonselective defects. By contrast, the growth of 3D COF films only involves the covalent bonds, and the interlaced pores are strategically avoided to give the predesignated structure. In our case, by integrating TFPM with long linear amines, the crystalline structure of 3D-OH-COF is prone to a multi-interpenetrated network.[33]

2.2. Preparation and Characterization of 3D-OH-COF Membranes. The CPI supports were prepared through nonsolvent-induced phase inversion method, followed by cross-linking using hexamethylenediamine (HDA) (Figure S6).[26] This produces the hyper-cross-linked supports with a mesoporous top layer, available for growing 3D-OH-COF under solvothermal conditions (Figure 2a). After the cross-linking and 3D-OH-COF growth, little changes in terms of the structure and porosity are observed for the support (Figures 2b and S7 and S8). The 24 h growth produces a continuous 3D-OH-COF layer with a thickness of ∼400 nm, exclusively located on the top surface (Figure S8). The occurrence of the cross-linking of PI is supported by the Fourier transform infrared (FTIR) spectra with the appearance of amide C═O and C−N and the obvious weakening of imide C═O and C−N (Figure 2c).[27] A new stretching signal at ∼1625 cm^{-1} assigned to imine bonds rationalizes the generation of 3D-OH-COF (Figures 2d and S9).[33] Because of the low thickness and excellent cohesion of 3D-OH-COF on CPI supports, the direct determination of its structural features is challenging. Accordingly, we performed the powder X-ray diffraction (PXRD), thermogravimetry, and N_2 adsorption−desorption measurements on the 3D-OH-COF powder collected along with the membrane preparation. Figure 2e shows that the 3D-OH-COF powder gives intense diffraction peaks at ∼6.08° and ∼12.5°, which can be assigned to the (200) and (101) crystal plane. The obtained PXRD pattern agrees well with the simulation and reported results,[33] suggesting a favorable

https://doi.org/10.1021/acs.nanolett.1c02919
Nano Lett. 2021, 21, 8355−8362

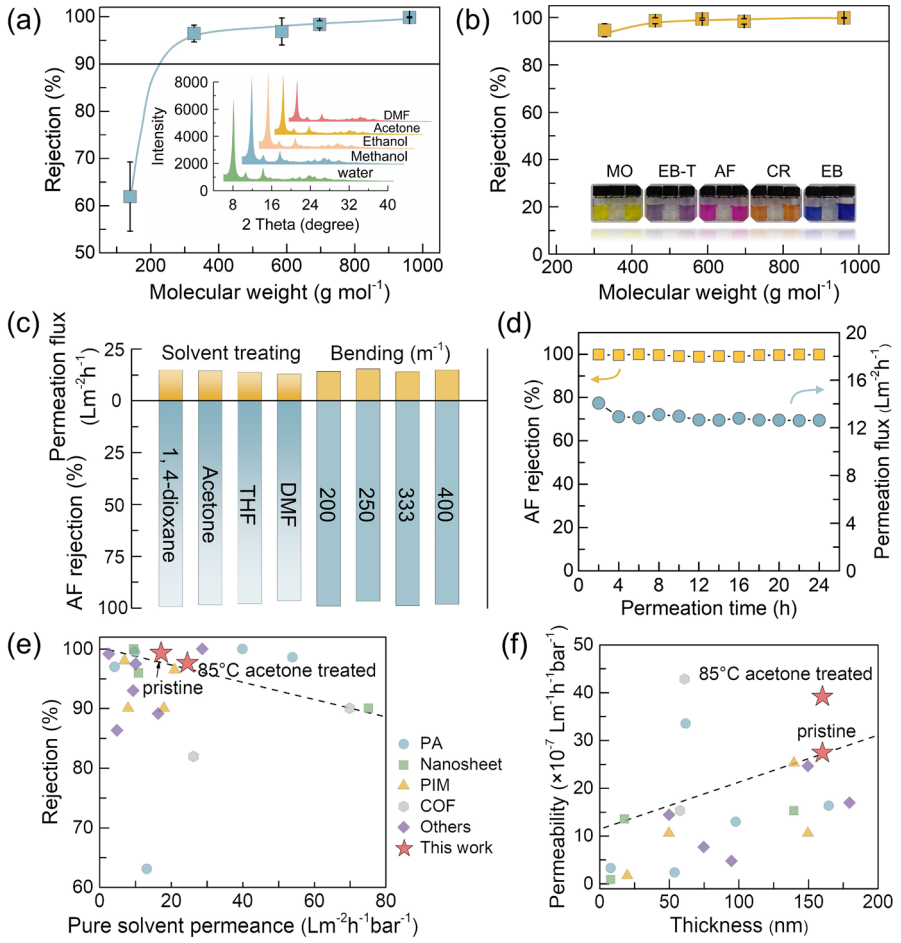

Figure 3. Performance of the 3D-OH-COF membrane synthesized for 6 h. (a,b) Rejection curves of the membrane for various molecules in water and methanol. (c) Performances of the membrane after solvent soaking and bending. (d) Long-term stability of the membrane in methanol. (e,f) Performance comparison between our membranes and others in literature. Insets in (a,b) are the XRD patterns of 3D-OH-COF powders after solvent treating for 1 week and the photograph of the solutions showing the colors of the feed, permeate, and retentate, respectively.

crystalline structure. Thermogravimetric analysis reveals that 3D-OH-COF can sustain a thermal treatment of up to ~450 °C (Figure S10). Further, the Brunauer−Emmett−Teller (BET) surface area is determined to be ~843.4 m^2 g^{-1}, and the nonlocal density functional theory (NLDFT) fitting recognizes a narrow pore size distribution centered at ~0.88 nm (Figure 2f). Considering that 3D-OH-COF grown on CPI supports experienced a completely same synthetic procedure to the powder, we reason that they own an identical crystalline structure. Compared to other COF membranes produced under mild conditions,[12,15] 3D-OH-COF synthesized in this work apparently has much higher crystallinity. The result manifests a superior pore uniformity benefiting for the size-dependent separation.

2.3. Molecular Separation by 3D-OH-COF Membranes. Seeking to comprehensively assess the performance of the 3D-OH-COF membranes, we explored the permeance and selectivity in water and organic solvents by dead-end filtration. The membrane synthesized for 6 h was chosen for these tests with the morphological features given in Figure S11. Clearly, the membrane presents a relatively rough surface (R_q ≈ 10 nm) with a 160 nm-thick 3D-OH-COF layer. The feasibility of 3D-OH-COF for liquid separation is evidenced by its remarkable stability in many solvents including acetone and *N*,*N*-dimethylformamide (DMF) (inset in Figure 3a, Figures S12 and S13). Figure S14 depicts the pure solvent permeance of the 3D-OH-COF membrane in water, ethanol, and methanol. Thereafter, the molecular weight cutoff (MWCO) of the membrane in water is estimated from the rejections to various molecules (Figure S15). In particular, the 3D-OH-COF membrane exhibits high rejections above 95% to molecules with a molecular weight >300 g mol^{-1} and a low rejection (~62%) to *p*-nitrophenol (NP, ~139.1 g mol^{-1}), thereby giving a MWCO of around 220 g mol^{-1} (Figure 3a). The MWCO value is greatly lower than that of other 2D COF-based membranes,[7] implying the sharp selectivity of 3D-OH-COF. Analogously, the membrane shows high rejections to dye molecules in methanol (Figure 3b). In these filtration tests, noticeable increases for the concentrations of all retention solutions exclude the influence of adsorption (Figures S16 and S17).

In the light of the polymer nature of both 3D-OH-COF and CPI, it is likely that the resulting membrane possesses a notable flexibility. To confirm this, a variety of toughness tests were explored by bending the membranes under different curvatures. Impressively, the treatment under the curvatures ranging from 200 to 400 m^{-1} causes no visible cracks, fragmentation, or detachment of the 3D-OH-COF layer (Figures S18 and S19). Moreover, the integrity of the membrane is kept intact after being folded, curled, and

https://doi.org/10.1021/acs.nanolett.1c02919
Nano Lett. 2021, 21, 8355−8362

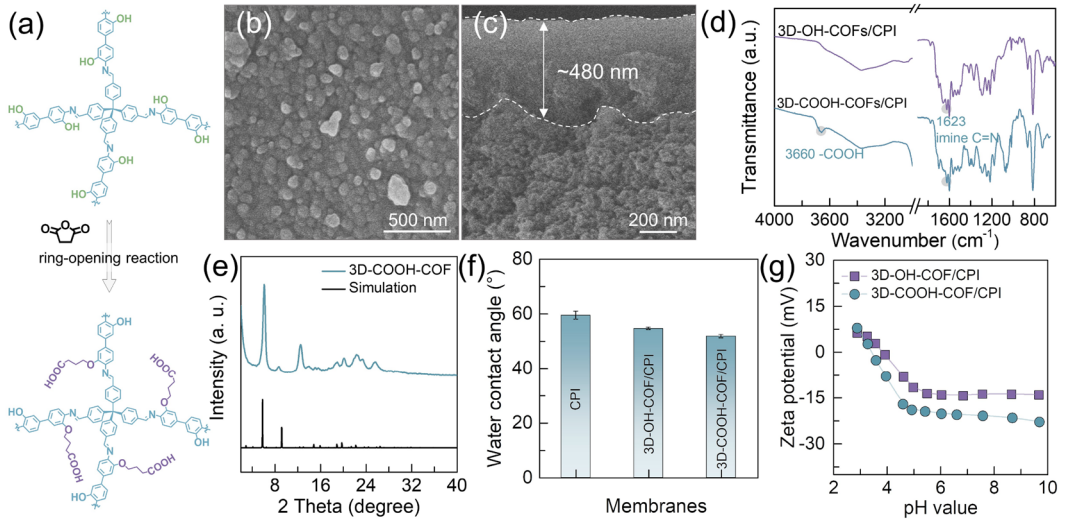

Figure 4. Preparation and characterization of the 3D-COOH-COF membrane. (a) Schematic diagram of the chemical conversion. (b,c) Surface and cross-sectional SEM images of the membrane. (d) FTIR spectra of the 3D-OH-COF and 3D-OH-COF membranes. (e) Experimental and simulated XRD patterns of the 3D-COOH-COF powder. (f,g) Water contact angles and Zeta potential curves of the membrane before and after the conversion.

unfolded, indicating the good flexibility (Figure S20). This excellent mechanical strength can be mostly ascribed to the use of robust CPI supports. To elucidate the chemical stability, the 3D-OH-COF membranes were immersed into aggressive solvents for 4 days at room temperature. The digital and SEM images taken after the soaking treatment show no structural damages for all of these membranes (Figures S21 and S22). We next checked the separation performance of the 3D-OH-COF membranes subjected to those tortures. Markedly, these membranes retain the original permeation flux and acid fuchsin (AF, ~585.5 g mol^{-1}) rejection (Figure 3c). Results of these definitely validate an enormous robustness of our membranes, making them a competent candidate to be operated under harsh conditions. In addition, a continuous 24 h filtration test without a significant variation in the performance suggests a prominent durability (Figure 3d). For some special purposes, the adopted membranes should endure both solvents and high temperatures.[34,35] The stability of 3D-OH-COF membranes in hot solvents heated to 85 °C was then studied, and negligible macroscopical changes can be noticed (Figure S23). Interestingly, the permeation fluxes are appreciably improved without sacrificing the selectivity after soaking in hot 1,4-dioxane and acetone (Figure S24). In detail, the membrane subjected to 85 °C acetone gains an improved flux of up to ~24.5 L m^{-2} h^{-1} while keeping a high AF rejection rate of ~97.7%. The performance increase possibly benefits from the removal of a few unreacted monomers and oligomers pre-adsorbed in 3D-OH-COF pores. The elimination of these obstacles opens more unimpeded mass transfer routes, thus promoting the solvent permeation while repelling the solutes. Compared with the conventional polymer- and nanosheet-based membranes suffering from the intractable swelling problem,[36,37] the 3D-OH-COF membrane exhibits an evident advantage in operating under extreme conditions. More importantly, the separation performance of our membranes outperforms most of the previously reported membranes built of polyamide, nanosheets, and others (Figure 3e,f and Table S1). This superiority can be traced to the fact that 3D-OH-COF has a narrow pore size distribution and a micropore-enriched skeleton, which consequently elevates the separation precision and efficiency.

Encouraged by above results, we explored the synthesis of the membranes based on other well-known COFs, including TpPa, TpBD, and TFPB-BD (Figure S25). Likewise, the obtained membranes display continuous and defect-free COF layers (Figures S26 and S27) and exhibit decent separation performances in methanol (Figures S28 and S29). Results of these suggest the unversality of our strategy in synthesizing COF membranes for orgainc solvent nanofiltration (OSN).[38] Here, the ordinary solvent permeances could be potentially caused by the isolated mass transfer channels and random stacking of 2D COFs. The aligned 1D channels in 2D COFs theoretically possess a reduced resistance, benefiting the mass transfer. As for separations, the membranes are expected to separate the targets from mixtures. In this process, we expect that one can pass through the membrane freely, and the other one is effectively rejected. To improve the separation efficiency, we thereby should create additional pathways for the one that ought to penetrate through the membrane while still keeping the other one excluded.[39] The interpenetrated channels of 3D COFs agree well with this design concept, which allows the fast permeation of solvents while repulsing the solutes in our cases.

2.4. Chemical Conversion of 3D-OH-COF Membranes.

By virtue of the high crystallinity and abundant hydroxyl groups in 3D-OH-COF, we chemically converted it into the carboxyl-functionalized COF through a ring-opening reaction (Figure 4a).[40] As for the membrane, the conversion will generate the 3D-COOH-COF layers featuring shrunken pore sizes and carboxyl-decorated pore walls. The 3D-COOH-COF membrane exhibits an unaltered surface morphology (Figures 4b and S30), and the thickness of the 3D-COOH-COF layer is measured to be ~480 nm (Figure 4c). The emergence of the characteristic band of −COOH at ~3660 cm^{-1} and the reservation of C═N stretching vibration collectively support the generation of 3D-COOH-COF (Figure 4d). We found that the crystallinity of the 3D-COOH-COF powder obtained by chemically converting the 3D-OH-COF powder is substantially retained (Figure 4e). The result indicates that the

https://doi.org/10.1021/acs.nanolett.1c02919
Nano Lett. 2021, 21, 8355−8362

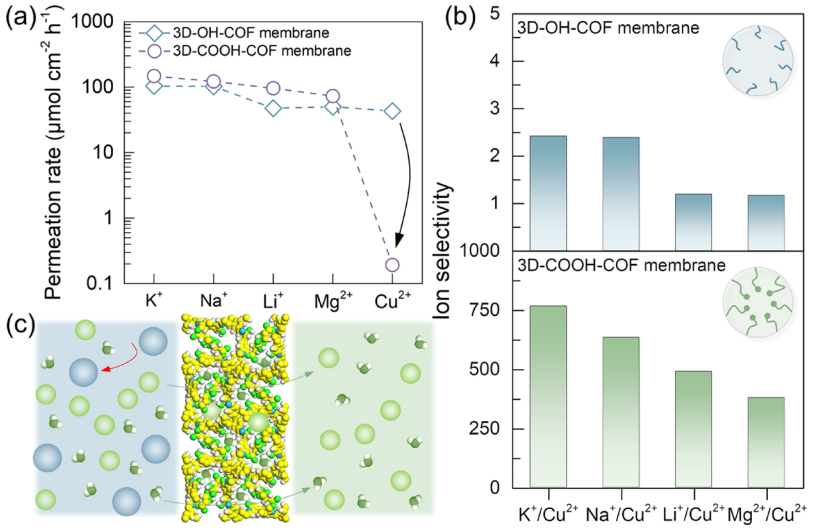

Figure 5. Ion capture of the 3D-COOH-COF membrane. (a,b) Ion permeation rates and corresponding selectivities of the membranes. (c) Schematic diagram of the selective ion capture by 3D-COOH-COF.

modification procedure gives negligible influences on the crystalline structure. With the formation of carboxyl-containing chains in the 3D-COOH-COF channels, we observe a substantial decrease in the BET surface area (~121.6 m^2 g^{-1}) and pore size (~0.8 nm) (Figure S31).[33] Also, the intrapore carboxyl groups raise the surface hydrophilicity and intensify the charge property (Figure 4f, g). Therefore, the aforesaid results prove a successful formation of 3D-COOH-COF on the top of CPI supports. The carboxyl-functionalized subnanometer channels would in return empower a heightened selectivity by the synergy of electrostatic repulsion and size exclusion.

2.5. Selective Ion Capture by 3D-COOH-COF Membranes. The competence of 3D-COOH-COF membranes toward ion capture was evaluated by selectively extracting monovalent ions from the ion mixture, as urgently desired in the extraction of special ions.[41] For these proof-of-concept studies, the tests were performed using a homemade diffusion cell, where pure water and ion solutions acted as the feed and draw solution, respectively (Figure S2). Figure S32 depicts a free permeation of all tested ions in the 3D-OH-COF membrane, accordingly illustrating a dye/salt separation capability (Figure S33). Moreover, it can be seen that the diffusion rates of various ions are in the same order of magnitude, verifying an inappreciable ion selectivity below 5 (Figure 5a,b). In sharp contrast, the 3D-COOH-COF membrane displays a largely reduced diffusion rate for Cu^{2+}, while the diffusion rates of the other ions keep basically unchanged (Figure S34). Consequently, the capture ability of the membrane for the target ion (Cu^{2+}) over competing ions is strongly improved upon the chemical conversion. For instance, the 3D-COOH-COF membrane exhibits exceptional selectivities of up to ~766, ~634, and ~490 for K^+/Cu^{2+}, Na^+/Cu^{2+}, and Li^+/Cu^{2+}, which exceed the results reported in literature.[42,43] The arresting improvement is rationalized by considering the combination of the interpenetrated angstrom-sized channels and specific pore environments (Figure 5c). Specifically, the three-dimensionally interconnected channels with subnanometer aperture sizes generate a confined space that selectively allows the penetration of small-size ions while excluding large-size ions like Cu^{2+}.[44] In addition, the terminal carboxyl groups in 3D-COOH-COF could serve as active sites to seize target ions through the chemical adsorption and electrostatic interaction.[45] Overall, the low energy consumption and high productivity make the 3D-COOH-COF membrane a promising candidate for the treatment of water containing heavy metal ions and even ion recovery. We further expect the design and synthesis of other multifunctional COFs and polymeric materials by the postsynthetic and predesign strategies for task-specific applications.

3. CONCLUSIONS

In summary, we have demonstrated the growth of high-crystallinity 3D-OH-COF on mesoporous CPI supports for flexible, tough molecular sieving membranes. The 3D-OH-COF membranes have a multi-interpenetrated network with prominent porosities and demonstrate a high-precision selectivity toward small molecules dispersed in both water and organic solvents. Because of the high crystallinity and polymer nature, as-fabricated 3D-OH-COF membranes exhibit a remarkable flexibility and excellent tolerance toward a wealth of extreme conditions (e.g., hot organic solvents). Subjected to the chemical conversion, the 3D-COOH-COF membrane bearing carboxyl-decorated pendants is further generated with unaltered crystallinity and narrowed aperture sizes. Compared to the mother membrane, they empower the selective capture of target ions over diverse competing ions. This work paves the way of producing high-quality COF membranes for precise separations under extreme environments and may inspire the profound study of distinctive 3D COFs in numerous areas.

■ ASSOCIATED CONTENT

Supporting Information

The Supporting Information is available free of charge at https://pubs.acs.org/doi/10.1021/acs.nanolett.1c02919.

Experimental procedures; diagram of the membrane holder and ion diffusion test; morphologies of 3D-OH-COF films and membranes; characterization on the 3D-OH-COF powder; solvent permeance of 3D-OH-COF membranes; dye rejection results; demonstration of flexibility and chemical stability; detailed information on

https://doi.org/10.1021/acs.nanolett.1c02919
Nano Lett. 2021, 21, 8355−8362

performance comparison; other COF structures and membrane performances; ion diffusion results (PDF)

AUTHOR INFORMATION

Corresponding Author

Yong Wang − *State Key Laboratory of Materials-Oriented Chemical Engineering, College of Chemical Engineering, Nanjing Tech University, Nanjing 211816 Jiangsu, P.R. China;* orcid.org/0000-0002-8653-514X; Email: yongwang@njtech.edu.cn

Authors

Xiansong Shi − *State Key Laboratory of Materials-Oriented Chemical Engineering, College of Chemical Engineering, Nanjing Tech University, Nanjing 211816 Jiangsu, P.R. China*

Zhe Zhang − *State Key Laboratory of Materials-Oriented Chemical Engineering, College of Chemical Engineering, Nanjing Tech University, Nanjing 211816 Jiangsu, P.R. China*

Siyu Fang − *State Key Laboratory of Materials-Oriented Chemical Engineering, College of Chemical Engineering, Nanjing Tech University, Nanjing 211816 Jiangsu, P.R. China*

Jingtao Wang − *School of Chemical Engineering, Zhengzhou University, Zhengzhou 450001 Henan, P.R. China;* orcid.org/0000-0002-2004-9640

Yatao Zhang − *School of Chemical Engineering, Zhengzhou University, Zhengzhou 450001 Henan, P.R. China;* orcid.org/0000-0002-6832-3127

Complete contact information is available at: https://pubs.acs.org/10.1021/acs.nanolett.1c02919

Author Contributions

The manuscript was written through contributions of all authors. All authors have given approval to the final version of the manuscript.

Notes

The authors declare no competing financial interest.

ACKNOWLEDGMENTS

This work was financially supported by the National Natural Science Foundation of China (21825803, 21921006). We also thank the Project of Priority Academic Program Development of Jiangsu Higher Education Institutions (PAPD).

REFERENCES

(1) Cote, A. P.; Benin, A. I.; Ockwig, N. W.; O'Keeffe, M.; Matzger, A. J.; Yaghi, O. M. Porous, Crystalline, Covalent Organic Frameworks. *Science* **2005**, *310* (5751), 1166−1170.

(2) Kandambeth, S.; Dey, K.; Banerjee, R. Covalent Organic Frameworks: Chemistry Beyond the Structure. *J. Am. Chem. Soc.* **2019**, *141* (5), 1807−1822.

(3) Ding, S.-Y.; Wang, W. Covalent Organic Frameworks (COFs): From Design to Applications. *Chem. Soc. Rev.* **2013**, *42* (2), 548−568.

(4) Guan, X.; Chen, F.; Fang, Q.; Qiu, S. Design and Applications of Three Dimensional Covalent Organic Frameworks. *Chem. Soc. Rev.* **2020**, *49* (5), 1357−1384.

(5) Yang, H.; Yang, L.; Wang, H.; Xu, Z.; Zhao, Y.; Luo, Y.; Nasir, N.; Song, Y.; Wu, H.; Pan, F.; Jiang, Z. Covalent Organic Framework Membranes through a Mixed-Dimensional Assembly for Molecular Separations. *Nat. Commun.* **2019**, *10*, 2101.

(6) Fan, H.; Peng, M.; Strauss, I.; Mundstock, A.; Meng, H.; Caro, J. MOF-in-COF Molecular Sieving Membrane for Selective Hydrogen Separation. *Nat. Commun.* **2021**, *12* (1), 1−10.

(7) Fan, H.; Gu, J.; Meng, H.; Knebel, A.; Caro, J. High-Flux Membranes Based on the Covalent Organic Framework COF-LZU1 for Selective Dye Separation by Nanofiltration. *Angew. Chem., Int. Ed.* **2018**, *57* (15), 4083−4087.

(8) Kandambeth, S.; Biswal, B. P.; Chaudhari, H. D.; Rout, K. C.; Kunjattu, S. H.; Mitra, S.; Karak, S.; Das, A.; Mukherjee, R.; Kharul, U. K.; Banerjee, R. Selective Molecular Sieving in Self-Standing Porous Covalent-Organic-Framework Membranes. *Adv. Mater.* **2017**, *29* (2), 1603945.

(9) Yuan, S.; Li, X.; Zhu, J.; Zhang, G.; Van Puyvelde, P.; Van der Bruggen, B. Covalent Organic Frameworks for Membrane Separation. *Chem. Soc. Rev.* **2019**, *48* (10), 2665−2681.

(10) Wang, H.; Wang, M.; Liang, X.; Yuan, J.; Yang, H.; Wang, S.; Ren, Y.; Wu, H.; Pan, F.; Jiang, Z. Organic Molecular Sieve Membranes for Chemical Separations. *Chem. Soc. Rev.* **2021**, *50*, 5468−5516.

(11) Wang, R.; Shi, X.; Xiao, A.; Zhou, W.; Wang, Y. Interfacial Polymerization of Covalent Organic Frameworks (COFs) on Polymeric Substrates for Molecular Separations. *J. Membr. Sci.* **2018**, *566*, 197−204.

(12) Wang, R.; Shi, X.; Zhang, Z.; Xiao, A.; Sun, S.-P.; Cui, Z.; Wang, Y. Unidirectional Diffusion Synthesis of Covalent Organic Frameworks (COFs) on Polymeric Substrates for Dye Separation. *J. Membr. Sci.* **2019**, *586*, 274−280.

(13) Su, Y.-Y.; Yan, X.; Chen, Y.; Guo, X.-J.; Chen, X.-F.; Lang, W.-Z. Facile Fabrication of COF-LZU1/PES Composite Membrane Via Interfacial Polymerization on Microfiltration Substrate for Dye/Salt Separation. *J. Membr. Sci.* **2021**, *618*, 118706.

(14) Fan, H.; Mundstock, A.; Feldhoff, A.; Knebel, A.; Gu, J.; Meng, H.; Caro, J. Covalent Organic Framework-Covalent Organic Framework Bilayer Membranes for Highly Selective Gas Separation. *J. Am. Chem. Soc.* **2018**, *140* (32), 10094−10098.

(15) Zhang, Y.; Guo, J.; Han, G.; Bai, Y.; Ge, Q.; Ma, J.; Lau, C. H.; Shao, L. Molecularly Soldered Covalent Organic Frameworks for Ultrafast Precision Sieving. *Science Advances* **2021**, *7* (13), No. eabe8706.

(16) El-Kaderi, H. M.; Hunt, J. R.; Mendoza-Cortes, J. L.; Cote, A. P.; Taylor, R. E.; O'Keeffe, M.; Yaghi, O. M. Designed Synthesis of 3D Covalent Organic Frameworks. *Science* **2007**, *316* (5822), 268−272.

(17) Guan, X.; Ma, Y.; Li, H.; Yusran, Y.; Xue, M.; Fang, Q.; Yan, Y.; Valtchev, V.; Qiu, S. Fast, Ambient Temperature and Pressure Ionothermal Synthesis of Three-Dimensional Covalent Organic Frameworks. *J. Am. Chem. Soc.* **2018**, *140* (13), 4494−4498.

(18) Liu, X.; Li, J.; Gui, B.; Lin, G.; Fu, Q.; Yin, S.; Liu, X.; Sun, J.; Wang, C. A Crystalline Three-Dimensional Covalent Organic Framework with Flexible Building Blocks. *J. Am. Chem. Soc.* **2021**, *143* (4), 2123−2129.

(19) Gao, C.; Li, J.; Yin, S.; Lin, G.; Ma, T.; Meng, Y.; Sun, J.; Wang, C. Isostructural Three-Dimensional Covalent Organic Frameworks. *Angew. Chem., Int. Ed.* **2019**, *58* (29), 9770−9775.

(20) Gui, B.; Lin, G.; Ding, H.; Gao, C.; Mal, A.; Wang, C. Three-Dimensional Covalent Organic Frameworks: From Topology Design to Applications. *Acc. Chem. Res.* **2020**, *53* (10), 2225−2234.

(21) Qiao, Z.; Liang, Y.; Zhang, Z.; Mei, D.; Wang, Z.; Guiver, M. D.; Zhong, C. Ultrathin Low-Crystallinity MOF Membranes Fabricated by Interface Layer Polarization Induction. *Adv. Mater.* **2020**, *32* (34), 2002165.

(22) Zhao, Y.; Wei, Y.; Lyu, L.; Hou, Q.; Caro, J.; Wang, H. Flexible Polypropylene-Supported ZIF-8 Membranes for Highly Efficient Propene/Propane Separation. *J. Am. Chem. Soc.* **2020**, *142* (50), 20915−20919.

(23) Shi, X.; Xiao, A.; Zhang, C.; Wang, Y. Growing Covalent Organic Frameworks on Porous Substrates for Molecule-Sieving Membranes with Pores Tunable from Ultra- to Nanofiltration. *J. Membr. Sci.* **2019**, *576*, 116−122.

(24) Shinde, D. B.; Sheng, G.; Li, X.; Ostwal, M.; Emwas, A.-H.; Huang, K.-W.; Lai, Z. Crystalline 2D Covalent Organic Framework Membranes for High-Flux Organic Solvent Nanofiltration. *J. Am. Chem. Soc.* **2018**, *140* (43), 14342−14349.
(25) Gouzman, I.; Grossman, E.; Verker, R.; Atar, N.; Bolker, A.; Eliaz, N. Advances in Polyimide-Based Materials for Space Applications. *Adv. Mater.* **2019**, *31* (18), 1807738.
(26) Tang, M.-J.; Liu, M.-L.; Wang, D.-A.; Shao, D.-D.; Wang, H.-J.; Cui, Z.; Cao, X.-L.; Sun, S.-P. Precisely Patterned Nanostrand Surface of Cucurbituril N -Based Nanofiltration Membranes for Effective Alcohol-Water Condensation. *Nano Lett.* **2020**, *20* (4), 2717−2723.
(27) Davood Abadi Farahani, M. H.; Hua, D.; Chung, T.-S. Cross-Linked Mixed Matrix Membranes (MMMs) Consisting of Amine-Functionalized Multi-Walled Carbon Nanotubes and P84 Polyimide for Organic Solvent Nanofiltration (OSN) with Enhanced Flux. *J. Membr. Sci.* **2018**, *548*, 319−331.
(28) Zhang, M.; Cui, J.; Lu, T.; Tang, G.; Wu, S.; Ma, W.; Huang, C. Robust, Functionalized Reduced Graphene-Based Nanofibrous Membrane for Contaminated Water Purification. *Chem. Eng. J.* **2021**, *404*, 126347.
(29) Wang, R.; Wei, M.; Wang, Y. Secondary Growth of Covalent Organic Frameworks (COFs) on Porous Substrates for Fast Desalination. *J. Membr. Sci.* **2020**, *604*, 118090.
(30) Haase, F.; Lotsch, B. V. Solving the COF Trilemma: Towards Crystalline, Stable and Functional Covalent Organic Frameworks. *Chem. Soc. Rev.* **2020**, *49* (23), 8469−8500.
(31) Wang, H.; He, B.; Liu, F.; Stevens, C.; Brady, M. A.; Cai, S.; Wang, C.; Russell, T. P.; Tan, T. W.; Liu, Y. Orientation Transitions During the Growth of Imine Covalent Organic Framework Thin Films. *J. Mater. Chem. C* **2017**, *5* (21), 5090−5095.
(32) Kang, C.; Zhang, Z.; Wee, V.; Usadi, A. K.; Calabro, D. C.; Baugh, L. S.; Wang, S.; Wang, Y.; Zhao, D. Interlayer Shifting in Two-Dimensional Covalent Organic Frameworks. *J. Am. Chem. Soc.* **2020**, *142* (30), 12995−13002.
(33) Lu, Q.; Ma, Y.; Li, H.; Guan, X.; Yusran, Y.; Xue, M.; Fang, Q.; Yan, Y.; Qiu, S.; Valtchev, V. Postsynthetic Functionalization of Three-Dimensional Covalent Organic Frameworks for Selective Extraction of Lanthanide Ions. *Angew. Chem., Int. Ed.* **2018**, *57* (21), 6042−6048.
(34) Zhao, C.; Yu, X.; Da, X.; Qiu, M.; Chen, X.; Fan, Y. Fabrication of a Charged PDA/PEI/Al_2O_3 Composite Nanofiltration Membrane for Desalination at High Temperatures. *Sep. Purif. Technol.* **2021**, *263*, 118388.
(35) Nilsson, M.; Lipnizki, F.; Tragardh, G.; Ostergren, K. Performance, Energy and Cost Evaluation of a Nanofiltration Plant Operated at Elevated Temperatures. *Sep. Purif. Technol.* **2008**, *60* (1), 36−45.
(36) Kim, S.; Wang, H.; Lee, Y. M. 2D Nanosheets and Their Composite Membranes for Water, Gas, and Ion Separation. *Angew. Chem., Int. Ed.* **2019**, *58* (49), 17512−17527.
(37) Marchetti, P.; Solomon, M. F. J.; Szekely, G.; Livingston, A. G. Molecular Separation with Organic Solvent Nanofiltration: A Critical Review. *Chem. Rev.* **2014**, *114* (21), 10735−10806.
(38) Wu, M.-B.; Yang, F.; Yang, J.; Zhong, Q.; Koerstgen, V.; Yang, P.; Mueller-Buschbaum, P.; Xu, Z.-K. Lysozyme Membranes Promoted by Hydrophobic Substrates for Ultrafast and Precise Organic Solvent Nanofiltration. *Nano Lett.* **2020**, *20* (12), 8760−8767.
(39) Tan, Z.; Chen, S.; Peng, X.; Zhang, L.; Gao, C. Polyamide Membranes with Nanoscale Turing Structures for Water Purification. *Science* **2018**, *360* (6388), 518−521.
(40) Liu, C.; Jiang, Y.; Nalaparaju, A.; Jiang, J.; Huang, A. Post-Synthesis of a Covalent Organic Framework Nanofiltration Membrane for Highly Efficient Water Treatment. *J. Mater. Chem. A* **2019**, *7* (42), 24205−24210.
(41) Li, J.; Wang, X.; Zhao, G.; Chen, C.; Chai, Z.; Alsaedi, A.; Hayat, T.; Wang, X. Metal-Organic Framework-Based Materials: Superior Adsorbents for the Capture of Toxic and Radioactive Metal Ions. *Chem. Soc. Rev.* **2018**, *47* (7), 2322−2356.
(42) Zhang, M.; Zhao, P.; Li, P.; Ji, Y.; Liu, G.; Jin, W. Designing Biomimic Two-Dimensional Ionic Transport Channels for Efficient Ion Sieving. *ACS Nano* **2021**, *15* (3), 5209−5220.
(43) Wang, P.; Wang, M.; Liu, F.; Ding, S.; Wang, X.; Du, G.; Liu, J.; Apel, P.; Kluth, P.; Trautmann, C.; Wang, Y. Ultrafast Ion Sieving Using Nanoporous Polymeric Membranes. *Nat. Commun.* **2018**, *9*, 569.
(44) Joshi, R. K.; Carbone, P.; Wang, F. C.; Kravets, V. G.; Su, Y.; Grigorieva, I. V.; Wu, H. A.; Geim, A. K.; Nair, R. R. Precise and Ultrafast Molecular Sieving through Graphene Oxide Membranes. *Science* **2014**, *343* (6172), 752−754.
(45) Fu, L.; Yan, Z.; Zhao, Q.; Yang, H. Novel 2D Nanosheets with Potential Applications in Heavy Metal Purification: A Review. *Adv. Mater. Interfaces* **2018**, *5* (23), 1801094.

https://doi.org/10.1021/acs.nanolett.1c02919
Nano Lett. 2021, 21, 8355−8362